# Effect of Anisotropic Strain on the Crosshatch Electrical Activity in Relaxed GeSi Films

M. H. Gray,[1] J. W. P. Hsu,[2,*] L. Giovane,[3] and M. T. Bulsara[4]

[1]*Department of Physics, University of Virginia, Charlottesville, Virginia 22901*
[2]*Bell Laboratories, Lucent Technologies, Murray Hill, New Jersey 07974*
[3]*Fiber-Optic Communications, Agilent Technologies, San Jose, California 95131*
[4]*AmberWaves Systems Corporation, Salem, New Hampshire 03079*

(Received 6 October 2000)

The physical origin of the crosshatch electrical activity in relaxed GeSi films was studied using a near-field scanning optical microscope (NSOM). The contrast and patterns in the near-field photocurrent images depend on the polarization direction of the NSOM light. These results rule out composition nonuniformity, junction depth variation, and scanning artifacts as dominant sources of the contrast. Numerical calculations show that local changes in band structure due to strain fields of the misfit dislocations are responsible for the experimental observations.

DOI: 10.1103/PhysRevLett.86.3598 PACS numbers: 71.70.Fk, 07.79.Fc, 61.72.Hh, 73.50.Pz

The control of strain relief and defect generation is critical for growing good quality heteroepitaxial films. Because of lattice mismatch, misfit dislocations are necessarily present in relaxed films. To control and minimize the threading dislocation density, a composition grading method is often employed. The surfaces of these films display a distinct morphology, termed "crosshatch," with lines of small undulations parallel to the misfit dislocation directions, i.e., the two orthogonal $\langle 110 \rangle$ directions in cubic semiconductors. The crosshatch is characteristic of well-controlled low mismatch growth, with misfit dislocation gliding dominating over nucleation, and has been observed in many heteroepitaxial systems [1–4]. In addition to the surface topography, the crosshatch displays electrical activity, showing contrast in cathodoluminescence [2,4], electron beam induced current [1,2,5], and near-field photocurrent (NPC) images [6,7]. The origin of this observed contrast is not well understood. In this work, we used a near-field scanning optical microscope (NSOM) with linearly polarized light to perform local photocurrent experiments on relaxed GeSi films. The crosshatch NPC contrast displays a marked polarization dependence, which cannot be explained by composition nonuniformity, junction depth variation, or feedback errors in NSOM. Rather, the variation reflects local changes in the band structure arising from directionally dependent strain fields of the dislocations. These changes result in diattenuation (anisotropic absorption) and birefringence (anisotropic index). This conclusion was reached by comparing experimental results with numerical calculations.

The relaxed $Ge_{0.3}Si_{0.7}$ films were grown on Si(001) substrates in a graded manner by increasing Ge content at 10% per $\mu$m. The grading process reduces the density of threading dislocations to $\leq 5 \times 10^6$ cm$^{-2}$, with long misfit segments along $\langle 110 \rangle$ directions. No additional dislocations nucleate in the 1 $\mu$m uniform $Ge_{0.3}Si_{0.7}$ cap layer [8]. Strain fields from the underlying misfit dislocations affect the local growth rate, resulting in nonperiodic surface undulations (crosshatch) [1,9]. These samples have been comprehensively described elsewhere [1,5,8]. The samples used in this experiment were grown on $p$-type Si wafers with no intentional doping in the GeSi films. A 400 Å $n^+$ layer was grown on top by coevaporating Sb at a density of $10^{18}$ cm$^{-3}$, resulting in a near surface junction. When above band gap photons are absorbed, electrons and holes are excited. The built-in electric field sweeps the photogenerated carriers from the depletion region, resulting in a photocurrent [6]. The generation region is laterally confined to the NSOM aperture size ($\sim$100 nm) [10]. Moreover, the high resolution NPC signal comes from within the near surface region before the light spot diverges. This length scale is also determined by the aperture size [11]. A shear-force feedback mechanism is used to regulate tip-sample separation [12] so that a topographic image is acquired simultaneously with an image of the local near-field photocurrent (NPC).

A 670 nm wavelength laser diode was used as the NSOM source. The excitation energy is 1.85 eV, higher than the indirect band gap (0.98 eV) and below the direct band gap (3.1 eV) for $Ge_{0.3}Si_{0.7}$. The polarization state is set by a polarizer, a $\lambda/2$ wave plate, and fiber paddles. The fiber paddles are used to compensate for the birefringence in the fiber-tip system in order to achieve a linear output polarization, and the $\lambda/2$ wave plate allows us to rotate the orientation of the linear polarization by 90°. An "analyzer sample," consisting of a rotatable linear polarizer mounted on top of a Si photodiode, allows us to determine the output polarization direction and extinction ratio of the NSOM light. Cleaved fibers measured this way showed an extinction ratio of 5000:1. NSOM tips typically have extinction ratios of $\sim$40:1. After the polarization of the NSOM light was set, the GeSi film was exchanged with the analyzer sample without altering the fiber-tip system. Thus, the NSOM polarization direction is known. We aligned one of the $\langle 110 \rangle$ directions of the GeSi sample parallel to the direction of the linear polarization.

Figure 1 shows a representative 10 $\mu$m $\times$ 10 $\mu$m area of the crosshatch patterns on these films. Figures 1(a) and

 0031-9007/01/86(16)/3598(4)$15.00 

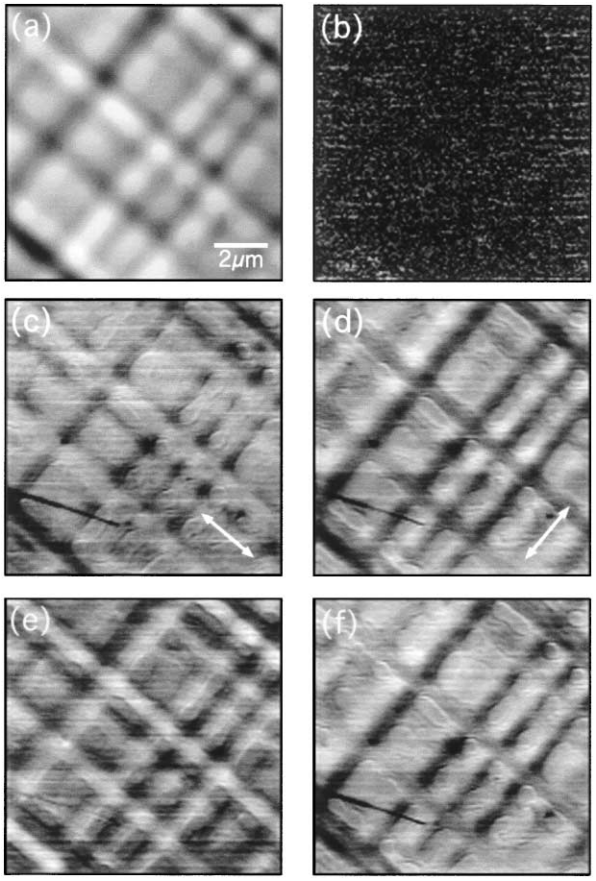


FIG. 1. NPC polarization dependence observed in crosshatch (scans are 10 $\mu$m $\times$ 10 $\mu$m). (a) A topographic image simultaneously acquired with NPC image (c). Gray scale in (a) is 300 Å. (b) The image resulting from a subtraction of the topographic image (not shown) taken simultaneously with (d) from (a). Gray scale in (b) is 15 Å. (c) An NPC image of the area with the polarization axis as indicated by the arrow ($-45°$ from the $+x$ axis). Variation in (c) is 3.13 to 3.26 nA. (d) An NPC image of the same area with the polarization rotated by 90°. Variation in (d) is 3.15 to 3.33 nA. (e) shows percent contrast in (c) minus the percent contrast of (d). The variation in (e) is 4.8% contrast. Image (f) is the set produced by averaging the percent contrast of (c) and (d). Variation in (f) is 4% contrast. (e) shows the polarization dependent part while (f) shows the polarization independent part of the NPC crosshatch contrast.

1(c) are simultaneously acquired topography and NPC, respectively (polarization $-45°$). Immediately after the scan, we rotated the polarization direction by 90° and took another image of the same area. Figure 1(d) shows the NPC image of the second scan. The difference in the topographic images associated with the two orthogonal polarization scans is shown in Fig. 1(b). The complete lack of features in Fig. 1(b) confirms that there was no drift in the piezo between these two scans. While the topography is the same, there are very clear differences in the polarized NPC images. A particularly striking example is a band running diagonally down from the top left to the lower right corner. In Fig. 1(c), the band is bright (enhanced NPC signal), while in Fig. 1(d) the same band is dark (reduced NPC signal). These results clearly show that the crosshatch NPC contrast depends on the *direction* of the linearly polarized light. The difference between NPC images taken with the two orthogonal polarizations [Figs. 1(c)–1(d)], normalized by the average NPC signal and expressed in percentage, is shown in Fig. 1(e). Figure 1(f) shows the average of the two, i.e., polarization independent part. The observed variation is 4.8% in Fig. 1(e) and 4.0% in Fig. 1(f). The explanation of the NPC crosshatch contrast will have to account for both polarization dependent and independent parts, as well as produce an effect on the same order of magnitude as is observed experimentally.

The results presented in Fig. 1 immediately eliminate some possible causes of the crosshatch electrical contrast. First, the contrast observed in 1(e) cannot arise from composition nonuniformity or junction depth variation since these do not produce polarization dependent effects. Second, the observed NPC contrast is not due to changes in tip-sample separation during the scan of a nonflat surface. While tip-sample separation can vary from position to position, Fig. 1(b) shows that the two topographic scans are identical so that, at a given position, the tip-sample separation is identical between the two scans. Hence, any contrast caused by the feedback error would be the same in both images and would not be present in the difference NPC image [Fig. 1(e)].

The NPC signal depends on carrier generation, diffusion, and recombination. Since the latter two processes do not depend on the polarization direction, the observed polarization dependence must come from the carrier generation, or light absorption, process. The first effect we will consider is the difference in transmission, hence, absorption, for $s$ and $p$ polarization caused by the nonflat surface morphology. Consider a light beam striking vertically a surface that is at an angle $\theta$ from the horizontal plane [Fig. 2(a), inset]. The polarization direction of the $s$ polarized light is out of the page and perpendicular to the slope and that of the $p$ polarized light is in the page and has a field component parallel to the slope. Figure 2(a) is a topographic line cut taken from Fig. 1(a) that shows the encountered surface angles $\leq 2.5°$. Using Fig. 2(a) and assuming light incident normal to the horizontal plane, the transmission difference between $s$ and $p$ polarizations is shown in Fig. 2(b) using the refractive index of relaxed $Ge_{0.3}Si_{0.7}$ [13]. Clearly, even the maximum difference ($\sim 0.1\%$) is 1 order of magnitude smaller than the experimental values [Fig. 2(c)]. Furthermore, the calculated results [Fig. 2(b)] are mostly zero except at regions of large slopes, clearly different from the measured NPC profile [Fig. 2(c)] which appears more like the topographic changes [Fig. 2(a)].

Strain fields have been shown to be associated with crosshatch [1,4,9,14]. Their presence affects local band structure, resulting in index and/or absorption variation. Since the dislocation strain fields are not isotropic, these changes can depend on direction. For polarization in the

⟨110⟩ directions, the measurement is most sensitive to changes in the $L$ valleys in the ⟨111⟩ directions ($E_L$ = 1.55 eV). In order to explore whether strain is the origin of the observed polarization dependence, we perform a numerical study. In this model, the number of 60° misfit dislocations necessary to achieve complete lattice strain relaxation is put into the 3 $\mu$m graded layer in two orthogonal ⟨110⟩ directions. Their positions and directions of Burgers vectors are assigned randomly to simulate heterogeneous nucleation [1]. The dislocations are assumed to span the entire length (45 $\mu$m) of the calculation area. Since the high resolution NPC signal comes from near surface regions [6,7], we evaluate the stress tensor $\overline{\overline{\sigma}}$ as a function of position at the sample surface plane (1 $\mu$m above the graded layer). This is done by summing over the stress components due to individual dislocations with the proper boundary conditions for a free boundary [15,16]. Strain is calculated from stress using the elastic stiffness ($C_{ij}$) of $Ge_{0.3}Si_{0.7}$ [17]. The shifts in the $L$ minima ($\Delta E_L$) are then obtained from the Ge deformation potential and the strain tensor [18]:

$$\Delta E_L = \hat{n}_L \cdot \{E_1(\varepsilon_{11} + \varepsilon_{22} + \varepsilon_{33})\overline{\overline{1}} + E_2[\overline{\overline{\varepsilon}} - \tfrac{1}{3}(\varepsilon_{11} + \varepsilon_{22} + \varepsilon_{33})\overline{\overline{1}}]\} \cdot \hat{n}_L ,$$

where $E_1$ and $E_2$ are the hydrostatic and shear deformation potentials, respectively, $\hat{n}_L$ is the unit vector in the direction of a given valley, $\overline{\overline{\varepsilon}}$ is the 3 × 3 strain tensor with components $\varepsilon_{ij}$, and $\overline{\overline{1}}$ is the unit dyadic. At a given location, the $L$ valley positions (fourfold degenerate in the absence of strain) vary because of differing strain in different ⟨111⟩ directions [19]. For polarization along a particular ⟨111⟩ direction, preferential absorption into the $L$ valley in that direction is assumed. Taking the $L$ valley position in that direction, the absorption coefficient ($\alpha_L$) is obtained [20]. For $Ge_{0.3}Si_{0.7}$ at 1.85 eV, the majority of absorption is due to $X$ valleys, which is assumed to be unaffected. The total absorption ($\alpha_{\text{total}}$) for $X$ and $L$ in the unstrained case is 5000 $\text{cm}^{-1}$ [21]. Figures 3(a) and 3(b) show 15 $\mu$m × 15 $\mu$m images of the calculated $\alpha_{\text{total}}$ for the two orthogonal polarization directions. Their difference and average, expressed in percentage change of $\alpha_{\text{total}}$, are shown in Figs. 3(c) and 3(d), respectively.

In addition to shifting the $L$ valleys, the stress changes the refractive index of the material. Anisotropic stress causes birefringence, resulting in different transmission coefficients for the two orthogonal polarizations. We calculate the birefringence from the stress tensors using the Si piezo-optic coefficients [22]. The image of the birefringence induced transmission difference is the same as Fig. 3(c). The diattenuation and birefringence effects contribute constructively to the NPC signal, i.e., the absorption and transmission are both higher at higher stress regions. The gray scale of the combined absorption and index difference between the two polarizations is

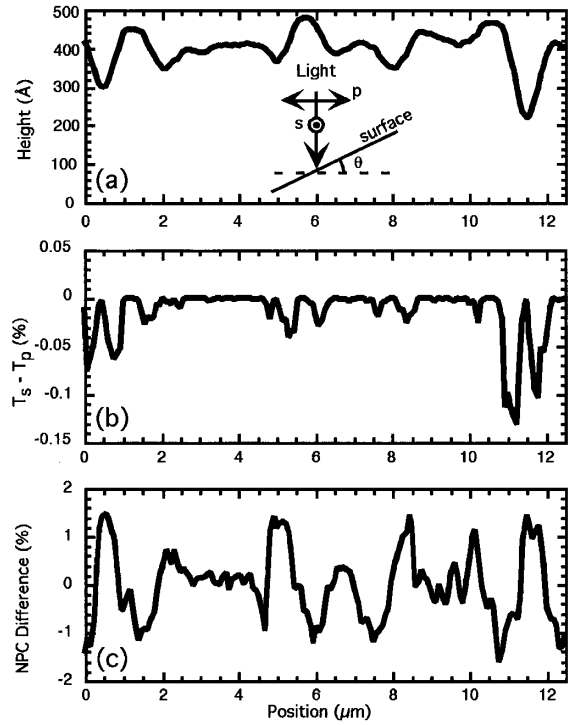


FIG 2. 12.5 $\mu$m line cuts of (a) topographic change [taken from Fig. 1(a)], (b) transmission difference between $p$ and $s$ polarizations calculated using (a), and (c) NPC difference between two orthogonal polarizations taken at the same positions as in (a) [taken from Fig. 1(e)].

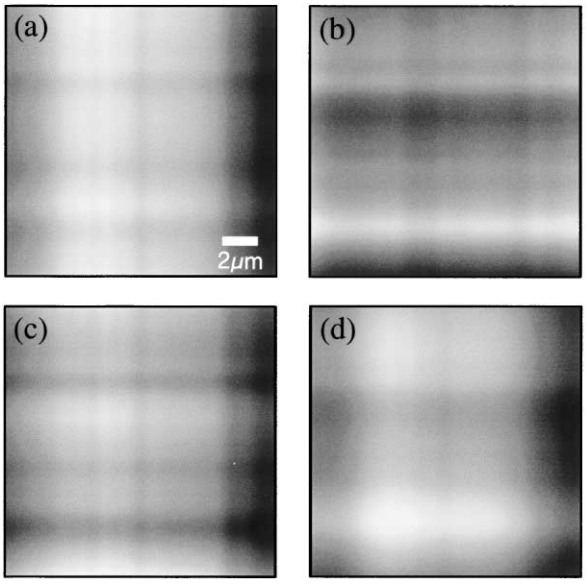


FIG. 3. 15 $\mu$m × 15 $\mu$m images of the calculated $\alpha_{\text{total}}$ for (a) horizontal and (b) vertical polarization. See text. The difference and average between (a) and (b) normalized to $\alpha_{\text{total}}$, expressed in percentage, are shown in (c) and (d), respectively. The variations are (a) 63 $\text{cm}^{-1}$, (b) 49 $\text{cm}^{-1}$, (c) 2.0%, and (d) 0.8%. The difference in transmittance experienced by the two polarizations has the same spatial variation as (c), with 0.6% contrast. Hence, the combined absorption and transmission difference image has a contrast of 2.6%.

~2.6% for the area shown in Fig. 3. This value is within a factor of 2 the measured NPC difference. Transmission electron microscopy study has shown that dislocations in crosshatch tend to bunch together, and the same Burgers vector is often found for neighboring dislocations [23]. Incorporation of this collective effect into our model would have produced larger strain variation, hence, higher calculated contrast and closer agreement with experiments. Furthermore, the enhanced and reduced absorption regions in the calculated image are similar in shape and period to the experimental results. Thus, we believe the dominant cause of the crosshatch electrical activity variation comes from local band structure change induced by dislocation strain fields.

Several approximations were used in our numerical model. Whenever possible, we interpolate the physical constants for $Ge_{0.3}Si_{0.7}$. However, the deformation potentials for $L$ valleys exist only for Ge and piezo-optic coefficients exist only for Si at this wavelength. The calculation of $\alpha_L$ assumes that the absorption occurs in the parabolic region of the conduction band, applicable here since the excitation energy is not much higher than $E_L$. We also assume complete preferential absorption when polarization is parallel to the stress direction. Since the strain fields are predominantly biaxial in the (001) plane, the valence band splitting affects only absorption with polarization in and out of the (001) plane, and therefore was not included in the calculation. Experimental measurements on strained Ge [24] agreed with both these assumptions. While these assumptions reduce the confidence level for the absolute value we obtain, the model can be trusted for order of magnitude estimation. Hence, we believe the physics concluded from the model is valid.

We performed polarized near-field photocurrent experiments and numerical calculations to investigate the origin of the crosshatch electrical contrast. Experimental results eliminate trivial explanations such as composition nonuniformity, junction depth variation, and scan artifacts. Difference in transmission of $s$ and $p$ polarized light due to nonflat topography also cannot account for the experimental observations. Numerical calculations show that observed NPC polarization dependence can be explained by dislocation strain fields. These fields cause directionally dependent $L$ valley shifts and produce birefringence, resulting in polarization dependent absorption and transmission. Hence, the intrinsic strain fields of the misfit dislocation network play a substantial role in the observed crosshatch electrical activity variation. While it has been shown that crosshatch surface morphology was linked to dislocation strain fields, this work provides definitive evidence that these strain fields cause spatially varying optoelectronic properties.

We thank E. A. Fitzgerald, Y. H. Xie, and P. J. Silverman for the samples, and V. Celli and F. Pollak for helpful discussion. This work is partially supported by DOE DE-FG02-98ER45679, and NSF DMR-9802634.

*Corresponding author.
Electronic address: jhsu@lucent.com

[1] E. A. Fitzgerald *et al.*, J. Vac. Sci. Technol. B **10**, 1807 (1992).
[2] E. A. Fitzgerald *et al.*, J. Appl. Phys. **63**, 693 (1988).
[3] Q. Xu *et al.*, J. Electron. Mater. **27**, 1010 (1998).
[4] K. Rammohan *et al.*, Appl. Phys. Lett. **66**, 869 (1995).
[5] E. A. Fitzgerald *et al.*, Appl. Phys. Lett. **59**, 811 (1991).
[6] J. W. P. Hsu *et al.*, J. Appl. Phys. **79**, 7743 (1996).
[7] M. H. Gray and J. W. P. Hsu, Appl. Phys. Lett. **76**, 1294 (2000).
[8] Y. H. Xie *et al.*, Mater. Sci. Eng. B **14**, 332 (1992).
[9] D. E. Jones *et al.*, Appl. Phys. Lett. **69**, 3245 (1996).
[10] Q. Xu, M. H. Gray, and J. W. P. Hsu, J. Appl. Phys. **82**, 748 (1997).
[11] M. Isaacson, J. Cline, and H. Barshatzky, Ultramicroscopy **47**, 15 (1992).
[12] J. W. P. Hsu, M. Lee, and B. S. Deaver, Rev. Sci. Instrum. **66**, 3177 (1995); M. Lee, E. B. McDaniel, and J. W. P. Hsu, Rev. Sci. Instrum. **67**, 1468 (1996).
[13] M. Klein and I. Furtak, *Optics* (Wiley, New York, 1986), Chap. 2.
[14] S. Y. Shiryaev *et al.*, Phys. Rev. Lett. **78**, 503 (1997); Y. H. Xie *et al.*, Appl. Phys. Lett. **71**, 3567 (1997).
[15] J. Weertman and J. Weertman, *Elementary Dislocation Theory* (Oxford University, Oxford, 1992), Chap. 2.
[16] J. Lothe, in *Elastic Strain Fields and Dislocation Mobility*, edited by V. L. Indenbom and J. Lothe (North-Holland, New York, 1992), Chap. 5.
[17] W. Kress, in *Semiconductors: Physics of Group IV Elements and III-V Compounds*, edited by O. Madelung, Landolt-Börnstein, New Series, Group III, Vol. 17a (Springer-Verlag, Berlin, 1982), pp. 63 and 105.
[18] F. H. Pollak, *Semiconductors and Semimetals*, edited by T. P. Pearsall (Academic, Boston, 1990), Vol. 32, Chap. 2.
[19] H. Brooks, *Advances in Electronics and Electron Physics*, edited by L. Marton (Academic, New York, 1955), Vol. 7, Chap. 2.
[20] J. Pankove, *Optical Processes in Semiconductors* (Prentice-Hall, Englewood Cliffs, NJ, 1971), Chap. 3.
[21] R. Braunstein, A. R. Moore, and F. Herman, Phys. Rev. **109**, 695 (1958).
[22] G. Harbeke, in *Semiconductors: Physics of Group IV Elements and III-V Compounds* (Ref. [17]), p. 72.
[23] S. Y. Shiryaev, F. Jensen, and J. W. Petersen, Appl. Phys. Lett. **64**, 3305 (1994).
[24] F. H. Pollak *et al.*, Inst. Phys. Conf. Ser. **43**, 867 (1979); O. J. Glembocki, Ph.D. dissertation, City University of New York, 1982.